

Accurate Evaluation of Interlaminar Stresses in Composite Laminates via Mixed One-Dimensional Formulation

*Original*

Accurate Evaluation of Interlaminar Stresses in Composite Laminates via Mixed One-Dimensional Formulation / de Miguel, A. G.; Carrera, E.; Pagani, A.; Zappino, E.. - In: AIAA JOURNAL. - ISSN 0001-1452. - STAMPA. - 56:11(2018), pp. 4582-4594. [10.2514/1.J057189]

*Availability:*

This version is available at: 11583/2715260 since: 2018-11-09T12:52:15Z

*Publisher:*

American Institute of Aeronautics and Astronautics

*Published*

DOI:10.2514/1.J057189

*Terms of use:*

openAccess

This article is made available under terms and conditions as specified in the corresponding bibliographic description in the repository

*Publisher copyright*

(Article begins on next page)

# Accurate evaluation of interlaminar stresses in composite laminates via mixed one-dimensional formulation

A.G. de Miguel<sup>\*1</sup>, E. Carrera<sup>†1</sup>, A. Pagani<sup>‡1</sup>, and E. Zappino<sup>§1</sup>

<sup>1</sup>Mul<sup>2</sup> Group, Department of Mechanical and Aerospace Engineering, Politecnico di Torino, 10129 Turin, Italy

This paper presents a novel mixed one-dimensional formulation based upon the Reissner's Mixed Variational Theorem (RMVT) for the accurate stress analysis of general multilayered beam problems. The Carrera's unified formulation (CUF) is recalled to generate a class of theory of structure that assumes both displacements and stresses over the cross-section of the beam. On the other hand, the finite element method (FEM) is employed to obtain the governing equations in weak form using standard Lagrangian interpolation. Independent assumptions are taken for each layer of the laminated beam through a Layer-Wise (LW) distribution of the unknowns and the interlaminar continuity of the transverse stresses is imposed a priori by ensuring piece-wise continuous fields in the thickness direction. A set of locally defined, hierarchical set of Legendre polynomials is chosen for the expansion of the variables over the cross-section surface, enabling the user to refine the model in particular zones of interest and to control the accuracy of the stress analysis through the polynomial order of the theory of structure. The numerical assessment of the proposed mixed elements for multilayered problems is carried out by comparison against benchmark solutions of the literature, including plate formulations and elasticity solutions. The free-edge problem is also addressed to show the 3D capabilities of the model.

## Nomenclature

$b$	=	width of the laminate
$C_{pp}, C_{nn}, C_{pn}, C_{np}$	=	stiffness matrices of the material
$D$	=	geometrical differential operator
$E$	=	Young's modulus
$F_\tau$	=	cross-section functions for displacements
$G$	=	shear modulus

---

<sup>\*</sup>Ph.D. Student, alberto.garcia@polito.it

<sup>†</sup>Professor of Aerospace Structures and Aeroelasticity, erasmo.carrera@polito.it

<sup>‡</sup>Assistant Professor, alfonso.pagani@polito.it

<sup>§</sup>Assistant Professor, enrico.zappino@polito.it

$G_\tau$	=	cross-section functions for stresses
$h$	=	thickness of the laminate
$\mathbf{K}_{uu}^{ij\tau s}, \mathbf{K}_{\sigma\sigma}^{ij\tau s}, \mathbf{K}_{u\sigma}^{ij\tau s}, \mathbf{K}_{\sigma u}^{ij\tau s}$	=	fundamental nuclei of the stiffness matrix
$k$	=	lamina index
$L$	=	length of the laminated beam
$L_e$	=	external work
$N_i$	=	Lagrangian 1D shape functions
$N_l$	=	number of layers
$n_{node}$	=	number of nodes of the beam element
$N_\tau$	=	number of expansion terms
$p_b$	=	polynomial order of the beam theory
$\mathbf{P}_\tau$	=	generalized force vector
$r, s$	=	natural coordinates of the section
$\mathbf{u}$	=	displacement vector
$\mathbf{u}_\tau$	=	generalized displacement vector
$V$	=	volume of the structure
$(x, y, z)$	=	coordinates of the reference system
$\delta$	=	virtual variation
$\boldsymbol{\varepsilon}_p, \boldsymbol{\varepsilon}_n$	=	in-plane and transverse strain vector
$\nu$	=	Poisson ratio
$\xi$	=	natural coordinate along the beam
$\boldsymbol{\sigma}_p, \boldsymbol{\sigma}_n$	=	in-plane and transverse stress vector
$\boldsymbol{\sigma}_{n\tau}$	=	generalized transverse stress vector
$\Omega$	=	cross-section surface

## I. Introduction

This paper proposes a computationally efficient modelling technique for general multilayered composite problems that is based on a one-dimensional finite element formulation derived via the Reissner's Mixed Variational Theorem (RMVT) [1]. The proposed formulation makes use of locally defined Legendre expansions which are mapped into the cross-section surface, allowing the user to hierarchically refine the beam's kinematics to a desired level of accuracy. The model can be applied to composite problems providing 3D stress fields throughout the structure with enriched solutions in the zones of interest.

The advantages of high-performance composites for structural applications are many, amongst them: high stiffness to weight ratio, high strength to weight ratio, fatigue strength, corrosion resistance or ease of formability, see the book of Tsai [2]. One of the most common form of composites are the multilayered structures, which are built by adding plies of the same or different materials in a certain stacking sequence to conform laminates with some desired characteristics. The layers are supposed to be perfectly bonded at the interfaces and can be made of metallic or composite materials. Due to these characteristics, multilayered structures exhibit some properties that differ from those of metallic structures, the first one being the transverse anisotropy, which is the variation of the mechanical properties through the thickness of the laminate. Also, the high values of orthotropic Young's modulus, being  $E_1/E_2 = E_1/E_3 = 5 \sim 40$ , where subscript 1 refers to the fiber direction of the ply, subscript 2 to the transverse in-plane direction and subscript 3 to the thickness direction, and low ratios of transverse shear moduli, being  $G_{12}/E_2 \approx G_{23}/E_2 = 1/10 \sim 1/200$ . Subsequently, the stress components in the thickness direction play a major role in the mechanical response and failure of laminated structures, therefore they should not be neglected in the structural model.

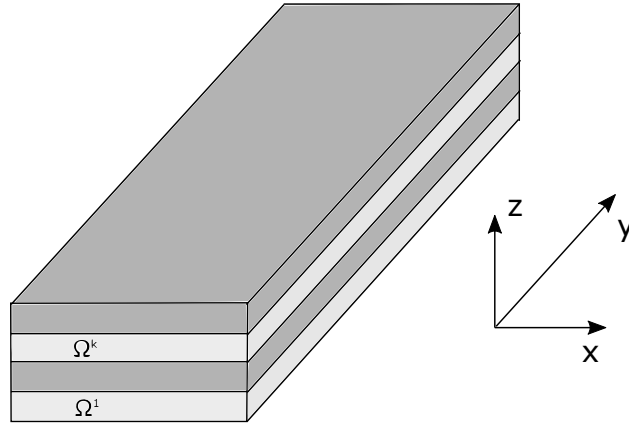


**Fig. 1 Reference system of a multilayered beam.**

The transverse anisotropy of multilayered materials leads to complex distributions of displacements, strains and stresses over the stacking direction. Following the notation introduced in Fig. 1, the fulfillment of the compatibility and equilibrium conditions requires continuous displacements ( $u_x, u_y, u_z$ ) and transverse stresses ( $\sigma_{zz}, \sigma_{xz}, \sigma_{yz}$ ) in the thickness direction, respectively. This requirement is referred to as Interlaminar Continuity (IC) and represents one of the major challenges in the modeling of laminated structures, see the book of Reddy [3] for instance. In order to satisfy the IC conditions, the slope of displacement fields must show a sudden change at interface between plies, which is commonly known as the zig-zag effect (ZZ). Fig. 2 illustrates the ZZ and IC requirements for a general multilayered structure. It is obvious then, that ZZ and IC conditions are strongly related to each other and must be correctly simulated to obtain an accurate description of the laminate response, as stated by Carrera [4]. Sumarizing, a proper model should include  $C^0$  displacements and  $C^0$  transverse stresses on the thickness direction at the same time. Nevertheless, these mechanical effects of laminated structures, which were generalized as the  $C_z^0$ -Requirements by Carrera [5], are not

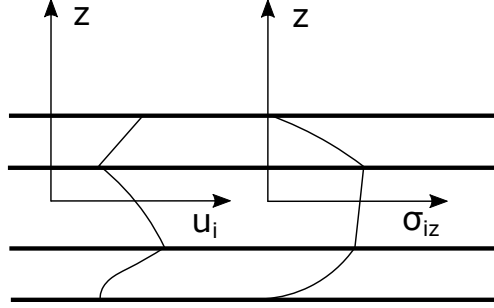


**Fig. 2 Typical displacement and transverse stress fields across the thickness of multilayered structures.**

fulfilled in the majority of the simulation tools available for composite design.

During the last decades, a vast amount of theories of structure have been introduced in the literature for the analysis of multilayered structures. The most commonly adopted models within the composite community are represented by the Classical Laminate Theories (CLT), see Jones [6], and the First-order Shear Deformation Theories (FSDT), such as those of Timoshenko [7], Reissner [8] or Mindlin [9], which are simplistic extensions of classical beam and plate theories for multilayered applications. Although these models are extensively accepted in composite design, one must be aware of the fact that the linear approximation adopted in these models for the displacement variables in the thickness direction leads, at the best, to a piece-wise constant distribution of the stress solutions, which are discontinuous at the interfaces between layers. Subsequently, the classical models cannot satisfy the IC conditions and the normal and transverse stresses can be only approximated to a short extent. Moreover, the necessity of shear correction factors, which are problem dependent and in many cases not easy to define, adds another limitation to these theories. An improvement of the CLT and FSDT models was introduced with the Higher-Order Theories (HOT), such as the higher-order model of Lo *et al.* [10], the Vlasov model [11] and the third-order shear deformation theory of Reddy [12], among others. In HOT, the polynomial order of the transverse assumptions for displacements is increased to account effects such as stress-free boundary conditions and warping of the cross-section, leading to models that are able to represent more complex deformations and stress fields.

All the aforementioned theories (CLT, FSDT and HOT) are categorized as Equivalent Single Layer (ESL) approaches, which provide acceptable global responses of the multilayered structure although do not address the  $C_z^0$ -Requirements. The first attempt to capture the ZZ effect was the introduction of the zig-zag theories, see Lekhnitskii [13], Ambartsumian [14] and Murakami [15]. These theories employ assumptions that vary from layer to layer so that the ZZ distributions are introduced in the kinematics. The ZZ conditions can also be satisfied if an independent approximation of the displacement variables is adopted for each layer. These models, introduced by Reddy [16], are referred to as Layer Wise (LW) and have been extensively studied in the literature, see for instance Pagano [17], Shimpi and Ghugal [18], Surana and Nguyen [19] and Carrera [20], among others. To this point, in these theories of structure the stress solutions are computed *a posteriori* via the Hooke's law and, therefore, the fulfillment of the IC for transverse stresses is not

guaranteed in a single step analysis. A second phase must be performed to recover the stresses from the 3D equilibrium for the IC to be satisfied, as proposed by Engrand [21], Noor and Burton [22] and Malik and Bert [23].

If both compatibility of the displacements and equilibrium conditions are to be satisfied without relying on post-processing methods to recover the stresses, assumptions on the stress fields must be taken. Reissner [1, 24, 25] restricted those assumptions to the transverse normal and shear stresses for the analysis of multilayered structures, leading to the so-called Reissner's Mixed Variational Principle. The RMVT solves the inconsistencies of displacement-based formulations for the computation of the 3D stress fields in multilayered structures and arises as a method to satisfy the  $C_z^0$ -Requirements completely and *a priori*. The most relevant developments of RMVT-based theories corresponds to the early works of Murakami [15], Toledano and Murakami [26], and Carrera [27–29]. The latter author introduced a unified formulation of theories of structure in which series of mixed and classical models could be arbitrarily generated and assessed. Further applications of the RMVT to multilayered structures can be found in Jing and Liao [30], Rao and Meyer-Piening [31], Carrera and Demasi [32], Wu and Li [33] and Tessler [34], among others. A comprehensive review of RMVT with plate/shell applications was presented by Carrera [35], in which a LW distributions of the stress variables are combined with different ESL, ZZ and LW theories. In the present research, a LW-LW approach is adopted by means of a hierarchical set of locally defined Legendre polynomials, ensuring the fulfillment of the  $C_z^0$ -Requirements automatically and with no need for ZZ terms in the kinematics or post-processing steps.

The paper is organized as follows: first, a general description of the RMVT is provided in Section II; then, Section III shows the derivation of RMVT-based theories of structure for beam structures by means of a unified formulation, and the definition of the polynomial basis used for the assumptions over the cross-section; subsequently, the obtention of the fundamental mathematical arrays of the problem for FEM applications is described in Section IV; the numerical assessment is presented in Section V; and finally, the conclusions are drawn in Section VI.

## II. Reissner's mixed variational theorem (RMVT)

In displacement-based formulations, the Principle of Virtual Displacements (PVD) uses compatible displacement fields as variables and establishes the equilibrium of internal and external work done by momenta and traction boundary conditions. The variational equation of PVD for static case reads

$$\int_V (\delta \boldsymbol{\epsilon}_p^T \boldsymbol{\sigma}_p + \delta \boldsymbol{\epsilon}_n^T \boldsymbol{\sigma}_n) dV = \delta L_e \quad (1)$$

where the variation of the internal work is split into in-plane components (subscript  $p$ ) and transverse components (subscript  $n$ ) for convenience reasons. Readily,  $\boldsymbol{\sigma}_p = \{\sigma_{xx}, \sigma_{yy}, \sigma_{xy}\}$ ,  $\boldsymbol{\epsilon}_p = \{\epsilon_{xx}, \epsilon_{yy}, \epsilon_{xy}\}$ ,  $\boldsymbol{\sigma}_n = \{\sigma_{zz}, \sigma_{xz}, \sigma_{yz}\}$  and  $\boldsymbol{\epsilon}_n = \{\epsilon_{zz}, \epsilon_{xz}, \epsilon_{yz}\}$ .  $\delta L_e$  refers to the virtual variation of the external work. The stress solutions are obtained *a posteriori* from the displacement solutions through the Hooke's law. Subsequently, the  $C_z^0$ -Requirements are not

guaranteed *a priori* and very refined theories are needed to obtain acceptable results. On the other hand, the fulfillment of IC conditions can be in some cases derived from a certain stress recovery method, which are in general based on the integration of the stress solutions in the 3D equilibrium equations, see Whitney [36].

The  $C_z^0$ -Requirements can be completely satisfied *a priori* if both displacement and stresses are used as variables in the variational principle. One way to achieve this is to make use of the Hu-Washizu principle [37], which imposes the compatibility conditions in the PVD through Lagrange multipliers. In the Hellinger-Reissner principle [38], on the other hand, the equilibrium of stresses is imposed as a constrain to the Principle of Virtual Forces through Lagrange multipliers. In these mixed variation principles, the Lagrange multipliers become the extra field of variables, i.e. stresses in the Hu-Washizu and displacements in the Hellinger-Reissner.

In multilayered structures, it is enough to impose the IC of stresses in the transverse direction. The RMVT is a variational formulation that enforces the  $C_z^0$ -Requirements *a priori* and completely through the use of independent fields for the displacement and stress variables. In RMVT-based formulations, the equilibrium of the transverse stresses are introduced in the PVD as follows:

$$\int_V (\delta \boldsymbol{\varepsilon}_{pG}^T \boldsymbol{\sigma}_{pH} + \delta \boldsymbol{\varepsilon}_{nG}^T \boldsymbol{\sigma}_{nM} + \delta \boldsymbol{\sigma}_{nM}^T (\boldsymbol{\varepsilon}_{nG} - \boldsymbol{\varepsilon}_{nH})) dV = \delta L_e \quad (2)$$

In this expression, subscript *H* refers to the evaluation of the variables through the Hooke's law, subscript *G* refers to the geometrical relations and subscript *M* denotes the use of assumed fields for the transverse stresses,  $\boldsymbol{\sigma}_{nM}$ . The reader can observe that fulfillment of the IC conditions is imposed by the compatibility of transverse strains obtained independently from the geometrical relations and the constitutive laws

$$\boldsymbol{\varepsilon}_{nG} = \boldsymbol{\varepsilon}_{nH} \quad (3)$$

In this manner, the RMVT principle enables the independent computation of the stresses that must be continuous in the thickness direction of the laminate, i.e.  $\sigma_{zz}, \sigma_{xz}, \sigma_{yz}$ , which become variables of the mechanical problem, and those that can be discontinuous at the interfaces due to the mismatch of the material properties of the plies, i.e.  $\sigma_{xx}, \sigma_{yy}, \sigma_{xy}$ , which are computed *a posteriori* through the Hooke's law.

## A. Constitutive relations

The laminates are assumed to deform in linear elastic range. For a generic  $k^{th}$ -lamina, the Hooke's law reads

$$\boldsymbol{\sigma}^k = \tilde{\mathbf{C}}^k \boldsymbol{\varepsilon}^k \quad (4)$$

Following the same notation of Eq. (1), the constitutive laws can be rewritten as

$$\begin{aligned}\sigma_{pH}^k &= \tilde{\mathbf{C}}_{pp}^k \boldsymbol{\varepsilon}_{nG}^k + \tilde{\mathbf{C}}_{pn}^k \boldsymbol{\varepsilon}_{nG}^k \\ \sigma_{nH}^k &= \tilde{\mathbf{C}}_{np}^k \boldsymbol{\varepsilon}_{pG}^k + \tilde{\mathbf{C}}_{nn}^k \boldsymbol{\varepsilon}_{nG}^k\end{aligned}\quad (5)$$

where the stiffness matrices for an orthotropic lamina read:

$$\begin{aligned}\tilde{\mathbf{C}}_{pp} &= \begin{bmatrix} \tilde{C}_{11} & \tilde{C}_{12} & \tilde{C}_{16} \\ \tilde{C}_{12} & \tilde{C}_{22} & \tilde{C}_{26} \\ \tilde{C}_{16} & \tilde{C}_{26} & \tilde{C}_{66} \end{bmatrix} & \tilde{\mathbf{C}}_{nn} &= \begin{bmatrix} \tilde{C}_{33} & 0 & 0 \\ 0 & \tilde{C}_{44} & \tilde{C}_{45} \\ 0 & \tilde{C}_{45} & \tilde{C}_{55} \end{bmatrix} \\ \tilde{\mathbf{C}}_{pn} &= \tilde{\mathbf{C}}_{np}^T = \begin{bmatrix} \tilde{C}_{13} & 0 & 0 \\ \tilde{C}_{23} & 0 & 0 \\ \tilde{C}_{36} & 0 & 0 \end{bmatrix}.\end{aligned}\quad (6)$$

In order to obtain the transverse strains from the Hooke's law,  $\boldsymbol{\varepsilon}_{nH}$ , it is possible to rewrite the constitutive relations as follows (see Carrera [35]):

$$\begin{aligned}\sigma_{pH}^k &= \mathbf{C}_{pp}^k \boldsymbol{\varepsilon}_{nG}^k + \mathbf{C}_{pn}^k \sigma_{nM}^k \\ \boldsymbol{\varepsilon}_{nH}^k &= \mathbf{C}_{np}^k \boldsymbol{\varepsilon}_{pG}^k + \mathbf{C}_{nn}^k \sigma_{nM}^k\end{aligned}\quad (7)$$

In these equations, the components of the constitutive matrices  $\mathbf{C}_{pp}^k$ ,  $\mathbf{C}_{pn}^k$ ,  $\mathbf{C}_{np}^k$  and  $\mathbf{C}_{nn}^k$  include both stiffness and compliance coefficients. They are obtained from the following relations:

$$\begin{aligned}\mathbf{C}_{pp}^k &= \tilde{\mathbf{C}}_{pp}^k - \tilde{\mathbf{C}}_{pn}^k \tilde{\mathbf{C}}_{nn}^{k-1} \tilde{\mathbf{C}}_{np}^k \\ \mathbf{C}_{pn}^k &= \tilde{\mathbf{C}}_{pn}^k \tilde{\mathbf{C}}_{nn}^{k-1} \\ \mathbf{C}_{np}^k &= -\tilde{\mathbf{C}}_{nn}^{k-1} \tilde{\mathbf{C}}_{np}^k \\ \mathbf{C}_{nn}^k &= \tilde{\mathbf{C}}_{nn}^{k-1}\end{aligned}\quad (8)$$

where  $\tilde{\mathbf{C}}_{nn}^{k-1}$  is the compliance matrix related to the transverse terms.



## B. Geometrical relations

For small displacements and rotations, displacements and strains are related to each other through the following geometrical relations:

$$\begin{aligned}\boldsymbol{\varepsilon}_{pG} &= \mathbf{D}_p \mathbf{u} \\ \boldsymbol{\varepsilon}_{nG} &= \mathbf{D}_n \mathbf{u}\end{aligned}\tag{9}$$

Accordingly, the differential operators  $\mathbf{D}_p$  and  $\mathbf{D}_n$  are written in explicit form as

$$\mathbf{D}_p = \begin{bmatrix} 0 & \frac{\partial(\bullet)}{\partial y} & 0 \\ \frac{\partial(\bullet)}{\partial x} & 0 & 0 \\ \frac{\partial(\bullet)}{\partial y} & \frac{\partial(\bullet)}{\partial x} & 0 \end{bmatrix} \quad \mathbf{D}_n = \begin{bmatrix} 0 & 0 & \frac{\partial(\bullet)}{\partial z} \\ \frac{\partial(\bullet)}{\partial z} & 0 & \frac{\partial(\bullet)}{\partial x} \\ 0 & \frac{\partial(\bullet)}{\partial z} & \frac{\partial(\bullet)}{\partial y} \end{bmatrix}\tag{10}$$

where  $\frac{\partial(\bullet)}{\partial}$  refers to the partial derivative with respect to the correspondent spatial coordinate.

## III. Unified formulation of beams via RMVT

Due to the geometrical features of multilayered structures, most RMVT-based theories of the literature deal with plate/shell applications, i.e. displacements and stresses are assumed only in the thickness direction. There are also a few works available on the implementation of mixed beam formulations via RMVT, see the works of Murakami *et al.* [39], Murakami and Yamakawa [40], and more recently Tessler [34], although to the authors best knowledge, they mostly deal with planar beam problems and exclude 3D effects such as double warping or free-edge effects. In order to address these physics into the model, this study extends the application of RMVT to 3D beam models.

Consider the Cartesian reference system shown in Fig. 1 for a laminated beam with an arbitrary number of layers,  $N_l$ , stacked in the thickness direction,  $z$ . The longitudinal axis of the beam corresponds to the coordinate  $y$  ( $0 \leq y \leq L$ ), whereas the cross-section, denoted by  $\Omega = \Omega^1 \cup \dots \cup \Omega^k \cup \dots \cup \Omega^{N_l}$ , lays on the  $xz$ -plane. Superscript  $k$  refers to the  $k^{th}$ -lamina. The Carrera's unified formulation [41] is recalled to generate a theory of structure that is suitable for the analysis of laminated beams. In the CUF framework, the assumed fields over the cross-section of the beam can take arbitrary forms, which are chosen by the user as an input of the analysis. Classical to ZZ, HOT, or LW theories can be defined arbitrarily by means of the same general formulation. In this line, Carrera *et al.* [42] made an interesting assessment of the use of different polynomial, trigonometric, exponential and zig-zag functions to enrich the kinematics of the assumed displacements over the cross-section. In the present work, a LW description of the displacement fields is assumed, which facilitates the fulfillment of the ZZ and IC conditions. Accordingly, the kinematics of the beam are

expressed as:

$$\mathbf{u}^k(x, y, z) = F_\tau(x, z) \mathbf{u}_\tau^k(y) \quad \tau = 1, 2, \dots, N_\tau; \quad k = 1, 2, \dots, N_l \quad (11)$$

where  $\mathbf{u}(x, y, z)$  is the three-dimensional displacement field,  $\mathbf{u}_\tau(y)$  is the vector of generalized displacements,  $N_\tau$  is the number of terms of the kinematic field and  $F_\tau(x, z)$  are the so-called expansion functions. According to the Einstein notation, repeated indexes denote summation.

In the same manner, the transverse stress variables are assumed over the cross-section in a LW sense, as follows

$$\sigma_{nM}^k(x, y, z) = G_\tau(x, z) \sigma_{nt}^k(y) \quad \tau = 1, 2, \dots, N_\tau; \quad k = 1, 2, \dots, N_l \quad (12)$$

A LW description of the transverse stresses is the natural choice due to the high gradients that they can exhibit through the stack of plies. The compatibility of the displacements and the IC requirement is imposed through the following relations

$$\begin{aligned} \mathbf{u}_t^k &= \mathbf{u}_b^{k+1} \\ \sigma_{nt}^k &= \sigma_{nb}^{k+1} \end{aligned} \quad (13)$$

for  $k = 1, N_l - 1$ . The subscripts  $t$  and  $b$  stand for top and bottom of the layer, respectively. In addition, this definition of the stress fields allows one to prescribe arbitrary stress boundary conditions *a priori* at the top and bottom faces of the laminated beam, as

$$\begin{aligned} \sigma_{nt}^{N_l} &= \sigma_{nt}^* \\ \sigma_{nb}^1 &= \sigma_{nb}^* \end{aligned} \quad (14)$$

where the superscript  $*$  denotes prescribed values. Subsequently, stress-free boundary conditions can be directly imposed in the analysis, as it will be shown in the numerical applications.

#### A. Theory of structure: Hierarchical Legendre Expansions

The characteristics of the CUF are exploited to generate a refined beam model which is suitable for the purposes of this implementation. For simplicity reasons, the same class of assumed functions are employed to expand the displacements and stress variables over the section of each ply of the laminate. A set of 2D Legendre-type polynomials, inspired from the work Szabó and Babuška [43] on the p-version of FEM, is constructed by adding hierarchically higher-order functions to the theory. The one-dimensional Legendre polynomials can be described in a recurrent manner

as follows:

$$\begin{aligned}
L_0 &= 1 \\
L_1 &= x \\
L_p &= \frac{2p-1}{p} x L_{p-1}(x) - \frac{p-1}{p} L_{p-2}(x), \quad p = 2, 3, \dots
\end{aligned} \tag{15}$$

Based on this set of polynomials, a hierarchial higher-order theory of structure was introduced first by Carrera *et al.* [44] and denoted to as Hierarchial Legendre Expansions (HLE). HLE displacement-based beam models were then applied to the analysis of multilayered beams by Pagani *et al.* [45].

In HLE models for RMVT applications, the expansion functions of the displacement and stress variables are defined in a natural domain  $[-1,1] \times [-1,1]$  and then mapped into the cross-section surface through a Jacobian transformation. This technique enables the discretization of the cross-section surface into an number of domains which is selected by the user.

The expansion functions of the first-order correspond to the vertex modes, which are defined as

$$F_\tau = \frac{1}{4}(1 - r_\tau r)(1 - s_\tau s) \quad \tau = 1, 2, 3, 4 \tag{16}$$

where  $r$  and  $s$  vary over the natural frame between  $-1$  and  $+1$ , and  $r_\tau$  and  $s_\tau$  represent the vertex coordinates of the quadrilateral domain. For the sake of simplicity, only the  $F_\tau$  expansions of the displacement assumptions are shown here, although the definition of the  $G_\tau$  assumed stresses is analogue. Subsequently, the expansion functions of higher-orders correspond to the side modes and the internal modes. The side modes are defined for  $p_b \geq 2$  and read:

$$F_\tau(r, s) = \frac{1}{2}(1 - s)\phi_{p_b}(r) \quad \tau = 5, 9, 13, 18, \dots \tag{17}$$

$$F_\tau(r, s) = \frac{1}{2}(1 + r)\phi_{p_b}(s) \quad \tau = 6, 10, 14, 19, \dots \tag{18}$$

$$F_\tau(r, s) = \frac{1}{2}(1 + s)\phi_{p_b}(r) \quad \tau = 7, 11, 15, 20, \dots \tag{19}$$

$$F_\tau(r, s) = \frac{1}{2}(1 - r)\phi_{p_b}(s) \quad \tau = 8, 14, 16, 21, \dots \tag{20}$$

where  $\phi_{p_b}$  corresponds to the one-dimensional internal Legendre-type modes, as described in [43]:

$$\phi_{p_b}(r) = \sqrt{\frac{2p_b-1}{p_b}} \int_{-1}^r L_{p_b-1}(x) dx, \quad p_b = 2, 3, 4, \dots \tag{21}$$

Finally, the internal modes are defined for  $p_b \geq 4$  and vanish at the edges of the quadrilateral domain. In total the

model includes  $(p_b - 2)(p_b - 3)/2$  internal functions for a given  $p_b$  order. The internal modes are then defined as:

$$F_\tau(r, s) = \phi_{p_1}(r)\phi_{p_2}(s) \quad p_b = p_1 + p_2, \quad (22)$$

The HLE model applied to multilayered structures with the RMVT principle present the following characteristics:

- It allows to generate LW theories straightforwardly with a direct imposition of the compatibility and equilibrium conditions at the interfaces via assembly into the stiffness matrix, according to (Eq. (13)).
- The accuracy of the model can be tuned through the polynomial order of the beam theory,  $p_b$ , which is introduced as a input parameter of the analysis.
- In complex problems with high gradients in the stress solutions, e.g. free-edge effects, the model allows the user to refine the discretization of HLE domains in the zones of interest over the cross-section, leading to a class of global-local h-refinement technique.

#### IV. Fundamental nuclei in FE applications

The governing equations of the RMVT method are derived in the weak form to obtain a new class of mixed beam elements. For this purpose, the displacement and transverse stress variables are written in terms of nodal unknowns and interpolated along the beam axis by means of standard 1D shape functions,  $N_i$ :

$$\begin{aligned} \mathbf{u}_\tau^k(y) &= N_i(y) \mathbf{u}_{\tau i}^k \quad i = 1, \dots, n_{node} \\ \boldsymbol{\sigma}_\tau^k(y) &= N_i(y) \boldsymbol{\sigma}_{\tau i}^k \quad i = 1, \dots, n_{node} \end{aligned} \quad (23)$$

where  $\mathbf{u}_{\tau i}^k = \{u_{\tau i x}^k, u_{\tau i y}^k, u_{\tau i z}^k\}$  and  $\boldsymbol{\sigma}_{\tau i}^k = \{\sigma_{\tau i x}^k, \sigma_{\tau i y}^k, \sigma_{\tau i z}^k\}$  are the displacement and transverse stress nodal unknowns, respectively. Cubic beam elements with equally spaced nodes are generated for all the numerical cases using Lagrangian shape functions:

$$\begin{aligned} N_1 &= -\frac{9}{16}(\xi + \frac{1}{3})(\xi - \frac{1}{3})(\xi - 1) \\ N_2 &= \frac{9}{16}(\xi + \frac{1}{3})(\xi - \frac{1}{3})(\xi + 1) \\ N_3 &= \frac{27}{16}(\xi + 1)(\xi - \frac{1}{3})(\xi - 1) \\ N_4 &= -\frac{27}{16}(\xi + 1)(\xi + \frac{1}{3})(\xi - 1) \end{aligned} \quad (24)$$

where the coordinate  $\xi$  varies along the domain  $[-1, 1]$ .

Introducing the FEM discretizations along the beam (Eq. (23)) and the expansions over the cross-section of the displacements (Eq. (11)) and the stresses (Eq. (12)), into the geometrical relations (Eq. (9)) and the Hooke's law in its

mixed form (Eq. (7)), respectively, one can rewrite the variational equations of the RMVT (Eq. (2)) as follows

$$\begin{aligned}
& \int_L \int_{\Omega} (\delta \mathbf{u}_{\tau i}^{kT} [\mathbf{D}_p^T (F_{\tau} N_i \mathbf{I}) \mathbf{C}_{pp}^k \mathbf{D}_p (F_s N_j \mathbf{I})] \mathbf{u}_{sj}^k + \\
& \delta \mathbf{u}_{\tau i}^{kT} [\mathbf{D}_p^T (F_{\tau} N_i \mathbf{I}) \mathbf{C}_{pn}^k (G_s N_j \mathbf{I}) + (F_{\tau} N_i \mathbf{I}) \mathbf{D}_n^T (G_s N_j \mathbf{I})] \boldsymbol{\sigma}_{sj}^k + \\
& \delta \boldsymbol{\sigma}_{\tau i}^{kT} [(G_{\tau} N_i \mathbf{I}) \mathbf{D}_n (F_s N_j \mathbf{I}) - (G_{\tau} N_i \mathbf{I}) \mathbf{C}_{np}^k \mathbf{D}_p (F_s N_j \mathbf{I})] \mathbf{u}_{sj}^k - \\
& \delta \boldsymbol{\sigma}_{\tau i}^{kT} [(G_{\tau} N_i \mathbf{I}) \mathbf{C}_{nn}^k (G_s N_j \mathbf{I})] \boldsymbol{\sigma}_{sj}^k) d\Omega dy = \delta L_e
\end{aligned} \tag{25}$$

where  $\mathbf{I}$  is the  $3 \times 3$  identity matrix. Equation (25) can be expressed in a compact form as

$$\delta \mathbf{u}_{\tau i}^{kT} [\mathbf{K}_{uu}^{k\tau sij} \mathbf{u}_{sj}^k + \mathbf{K}_{u\sigma}^{k\tau sij} \boldsymbol{\sigma}_{sj}^k] + \delta \boldsymbol{\sigma}_{\tau i}^{kT} [\mathbf{K}_{\sigma u}^{k\tau sij} \mathbf{u}_{sj}^k + \mathbf{K}_{\sigma\sigma}^{k\tau sij} \boldsymbol{\sigma}_{sj}^k] = \delta \mathbf{u}_{\tau i}^{kT} \mathbf{P}_{\tau i}^k \tag{26}$$

where  $\mathbf{K}_{uu}^{k\tau sij}$ ,  $\mathbf{K}_{u\sigma}^{k\tau sij}$ ,  $\mathbf{K}_{\sigma u}^{k\tau sij}$  and  $\mathbf{K}_{\sigma\sigma}^{k\tau sij}$  are the  $3 \times 3$  fundamental nuclei of the RMVT stiffness matrix. The formal expressions of the fundamental nuclei are independent on the choice of the cross-sectional functions  $F_{\tau}$  and  $G_{\tau}$ , which determine the theory of structure. This means that any classical to higher-order beam element can be automatically generated by opportunely expanding the fundamental nuclei according to the indexes  $\tau$ ,  $s$ ,  $i$ , and  $j$ . For the sake of completeness, the explicit expressions of the fundamental nuclei are included in Appendix A.

Finally, the governing equations of the RMVT in weak form can be written as

$$\begin{aligned}
\delta \mathbf{u}_{\tau i}^{kT} : \mathbf{K}_{uu}^{k\tau sij} \mathbf{u}_{sj}^k + \mathbf{K}_{u\sigma}^{k\tau sij} \boldsymbol{\sigma}_{sj}^k &= \mathbf{P}_{\tau i}^k \\
\delta \boldsymbol{\sigma}_{\tau i}^{kT} : \mathbf{K}_{\sigma u}^{k\tau sij} \mathbf{u}_{sj}^k + \mathbf{K}_{\sigma\sigma}^{k\tau sij} \boldsymbol{\sigma}_{sj}^k &= 0
\end{aligned} \tag{27}$$

## V. Results

The numerical assessment of the proposed mixed beam model is firstly carried out through comparison against benchmark solutions, including the elasticity results of Pagano [17] and refined plate and beam theories from the literature. Then, a 3D laminated beam under tensile loading is considered and the enhanced accuracy of the mixed beam elements to capture the complex effects at the free-edges is demonstrated. For the sake of clarity, within the proposed solutions the acronyms  $\text{HLM}p_b$  correspond to mixed HLE models based upon RMVT, whereas  $\text{HL}p_b$  refer to displacement-based HLE models.

### A. Laminates

Two thick laminates are chosen first to assess the stress solutions of the proposed mixed beam elements. The results are compared against three-dimensional exact solutions of Pagano [17, 46] and different LW and ESL models proposed

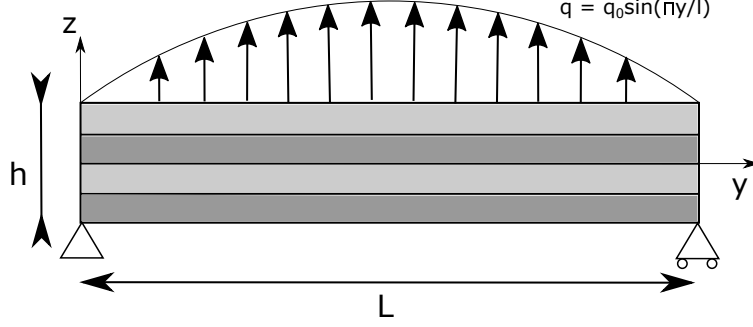


**Fig. 3 Loading case of the laminates.**

by Carrera [27, 47]. Figure 3 shows the characteristics of the case for a generic laminate. The slenderness ratio,  $L/h$ , is equal to 4 in all cases. A sinusoidal distributed load of a single wave is applied along the beam axis at the top face of the laminate, being its magnitude equal to  $q_0$ . The laminate is simply supported and cylindrical bending is imposed. A three-layer symmetric and four-layer anti-symmetric stacking sequences are studied. For both cases, the normalized material properties of the lamina are the following:

$$E_1/E_2 = 25, \quad G_{12}/E_2 = 0.5, \quad G_{23}/E_2 = 0.2, \quad \nu_{12} = \nu_{23} = 0.25 \quad (28)$$

with  $E_2 = 1$  MPa. Four cubic beam elements are placed along the longitudinal axis ( $y$  in correspondence with Fig. 3) and each lamina is represented by a single HLE domain over the cross-section. In this manner, once the model is set, the accuracy of the displacement and stress solutions can be *a priori* and axiomatically tuned by means of the polynomial order of the theory,  $p_b$ . In this assessment, linear (HLM1), quadratic (HLM2) and cubic (HLM3) Legendre expansions are considered.

Figures 4, 5 and 6 show the solutions of longitudinal, transverse normal and transverse shear stresses, respectively. Among the reference solutions, LWM4 corresponds to a forth-order LW expansions, whereas EMZC3 refers to a third-order ESL expansion with zig-zag function. Both solutions were obtained using plate elements also based upon RMVT [47]. The results are presented in normalized form according to the following criteria:

$$\bar{u}_y = u_y \times E_2 / (q_0 h) \quad \bar{\sigma}_{yy} = \sigma_{yy} / q_0 \quad \bar{\sigma}_{zz} = \sigma_{zz} / q_0 \quad \bar{\sigma}_{yz} = \sigma_{yz} / q_0 \quad (29)$$

The solutions of the anti-symmetric laminate are shown in Fig. 7, 8 and 9, accounting for normalized longitudinal displacements, transverse normal stresses and transverse shear stresses, respectively. The reference solutions are obtained from [27]. In that work, mixed formulations are indicated with M, displacement-based with D, (M) refers to stresses obtained *a priori*, (3D) correspond to stresses obtained *a posteriori* through integration of the 3D elasticity equilibrium equations, and (H) refer to stresses obtained through the Hooke's law. The solutions of the first-order (HL1)

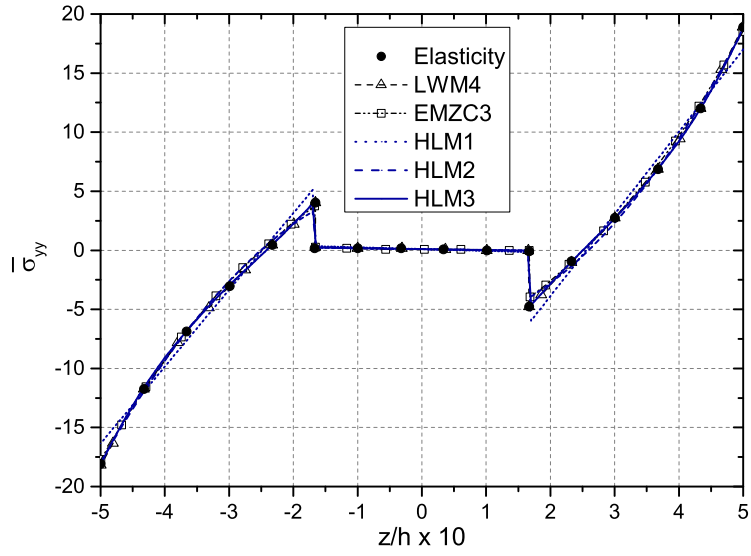


**Fig. 4** Longitudinal stress of the symmetric 3 layer laminate at  $y=L/2$ .

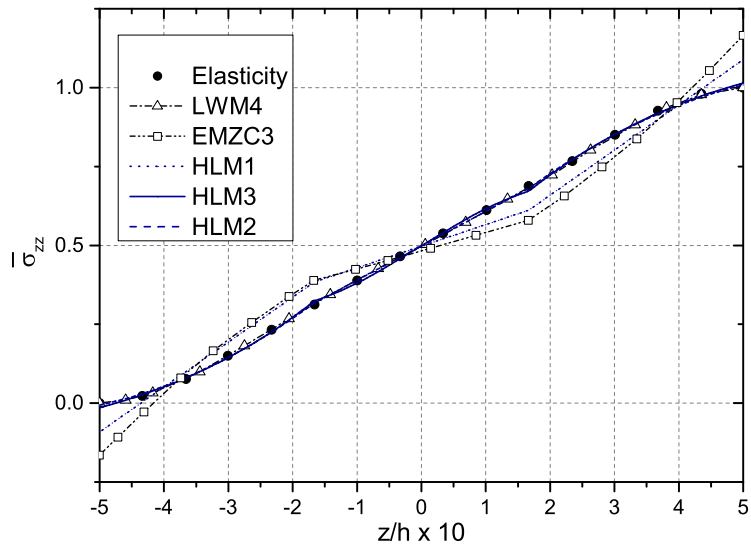


**Fig. 5** Transverse normal stress of the symmetric 3 layer laminate at  $y=L/2$ .

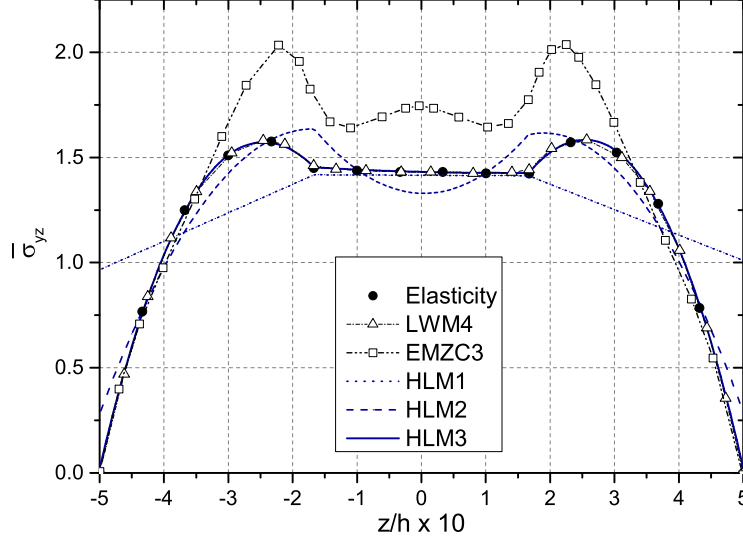


**Fig. 6** Transverse shear stress of the symmetric 3 layer laminate at  $y=0$ .

and second-order (HLM2) beam models based on the PVD, are also included in Fig. 9 for comparison purposes.

Both the ZZ and IC effects are fulfilled in all cases of mixed models, even when low-order expansions are employed. Indeed, one can notice that RMVT-based models provide always continuous solutions of the transverse stresses at the interface between layers independently of the accuracy of the stress fields. This effect cannot be represented by PVD-based models, which do not respect the  $C_z^0$ -Requirements and show highly discontinuous values of the interlaminar stresses, see Fig. 9. One can observe that by increasing the polynomial order of the stress fields in the mixed models, the transverse stress solutions converge to the 3D elasticity solutions. The second-order mixed model (HLM2) provides acceptable results in terms of transverse stresses, although the stress boundary conditions at top and bottom faces are not fully satisfied and the values at the interfaces differ from those of the references, see Fig.6 for instance. These errors are overcome with the third-order mixed model (HLM3), which shows very good agreement with the elasticity solutions.

Finally, in order to fully exploit the features of the proposed model, stress boundary conditions (Eq. (14)) are imposed at the top and bottom faces of the laminate in Fig. 10, which shows the transverse stress solutions for the symmetric (a) and anti-symmetric (b) laminates. In this case, the convergence to the elasticity solutions is clearly accelerated: the linear model (HLM1 SBC) provides fairly good solutions of the transverse shear stresses, which are exactly zero at the free faces and piece-wise continuous through the stacking sequence, whereas the quadratic model (HLM2 SBC) shows very small error in comparison to the elasticity solution.

## B. Composite sandwich

The second assessment deals with a symmetric sandwich beam with cross-ply skins. The features of the cases and the material properties are based on those of the work of Groh and Weaver [48]. The skins are made of carbon-fiber (cf) and the core is made of a symmetric sequence of polyvinyl chloride foam (pvc) and honeycomb (hc). The stacking



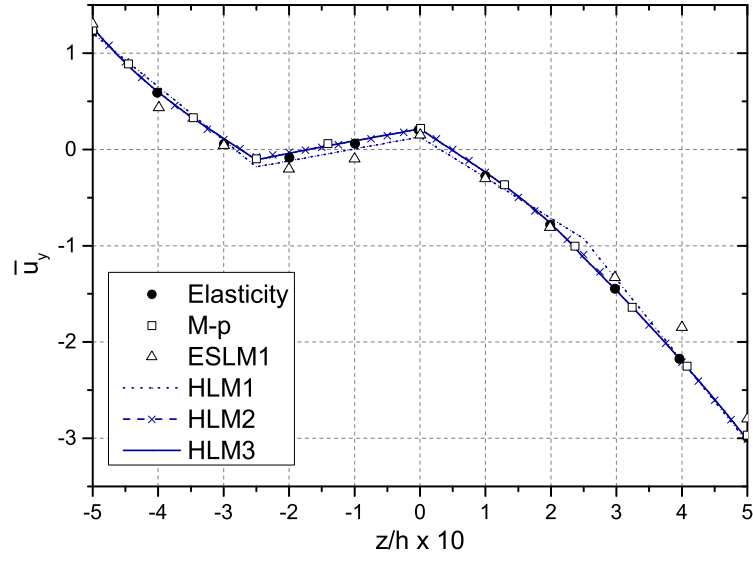


Fig. 7 Longitudinal displacements of the anti-symmetric laminate at  $y=0$ .

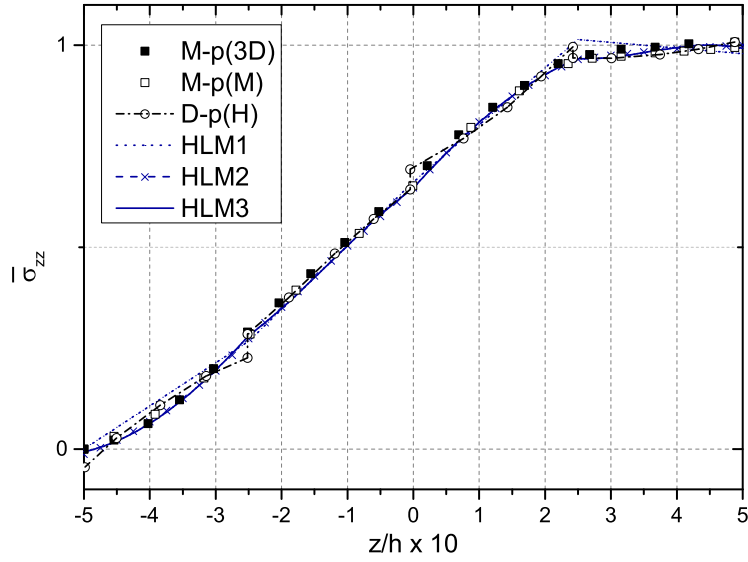
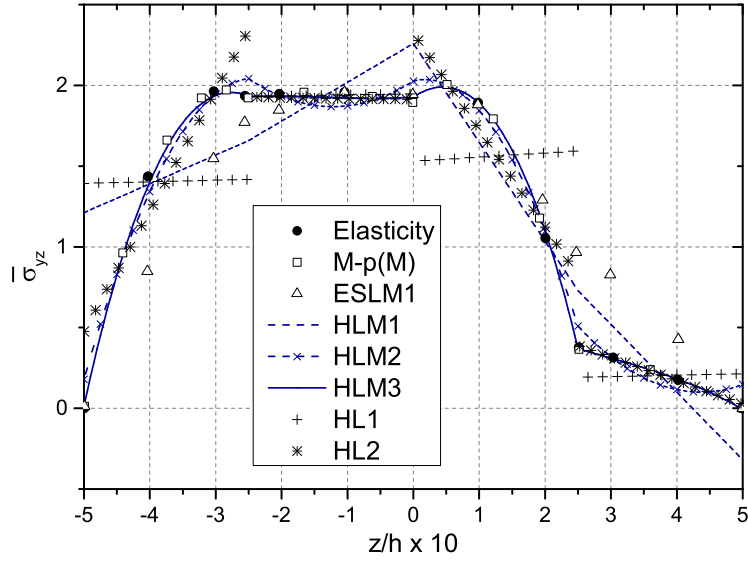
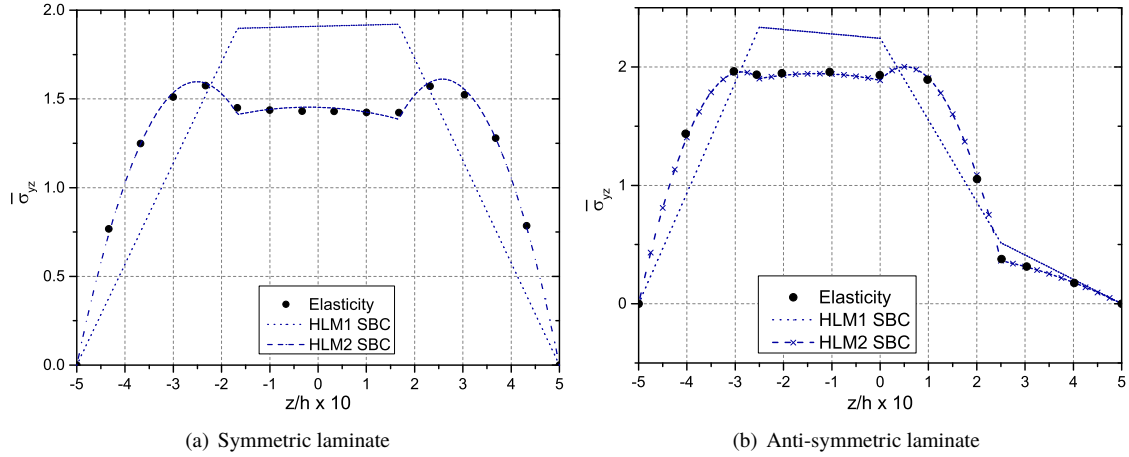


Fig. 8 Transverse normal stress of the anti-symmetric layer laminate at  $y=L/2$ .



**Fig. 9** Transverse shear stress of the anti-symmetric layer laminate at  $y=0$ .



**Fig. 10** Transverse shear stresses of the symmetric and anti-symmetric laminates with imposed stress-free boundary conditions.

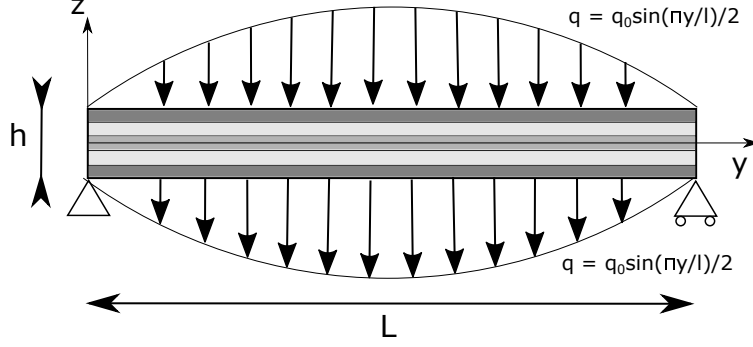


**Fig. 11 Loading case of the composite sandwich.**

sequence of the sandwich is  $[cf_{90}/cf_0/pvc/hc/pvc/cf_0/cf_{90}]$ , where the subindexes 0 and 90 refer to the fiber angle with respect to the  $y$ -axis. The geometry and loading case are illustrated in Fig. 11. Table 1 shows the material properties of the constituents normalized with respect to the shear moduli of the honeycomb,  $G_{12}^{(hc)}$ . The relative thickness of each layer is  $[0.1/0.1/0.2/0.2/0.2/0.1/0.1]$  and the slenderness ratio  $L/h$  is equal to 8. According to the authors of the original work [48], this particular numerical case represents a challenging test for structural models due to the high transverse anisotropy of the materials that compose the sandwich structure, which maximizes the ZZ effects, and the fact that externally weak layers ( $cf_{90}$ ) are placed at top and bottom faces. Distributed sinusoidal loads of a single wave and magnitude  $q_0/2$  are applied downwards in correspondence with the top and bottom faces and plane stress assumptions are imposed.

**Table 1 Mechanical properties of the materials for the composite sandwich example. The values of Young's moduli and shear moduli are normalized with respect to  $G_{12}$  of the honeycomb (hc).**

Material	$E_1$	$E_2$	$E_3$	$G_{12}$	$G_{13}$	$G_{23}$	$\nu_{12}$	$\nu_{13}$	$\nu_{23}$
cf	$25 \times 10^6$	$1 \times 10^6$	$1 \times 10^6$	$5 \times 10^5$	$5 \times 10^5$	$2 \times 10^5$	0.25	0.25	0.25
pvc	$25 \times 10^4$	$25 \times 10^4$	$25 \times 10^4$	$9.62 \times 10^6$	$9.62 \times 10^6$	$9.62 \times 10^6$	0.3	0.3	0.3
hc	250	250	2500	1	875	1750	0.9	$3 \times 10^{-5}$	$3 \times 10^{-5}$

The distribution of stress fields across the thickness at different locations along the beam axis are shown in Fig. 12, 13 and 14. The solutions from the reference paper correspond to a refined zig-zag theory inspired in the work of Tessler *et al.* [49] and are based upon the Hellinger-Reissner variational principle (HR-RZT), a modified third-order theory accounting for zig-zag effects (MRZZ) and RMVT-based zig-zag model (RMVT-RZT). The 3D elasticity solutions of Pagano [17] are also included. All the reference data has been extracted directly from the published graphs. As for the previous numerical examples, four cubic beam element are used along the longitudinal direction and each layer of the sandwich is represented by a single HLE domain.

The results show that the proposed LW-LW mixed beam model is able to provide acceptable solutions already for the second-order model (HLM2) and the convergence to the 3D elasticity is reached for the third-order model (HLM3).

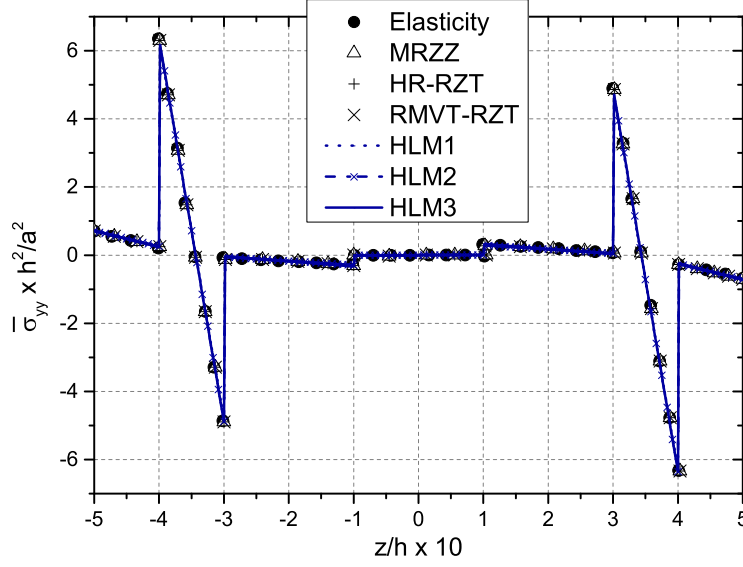


**Fig. 12** Longitudinal stress of the composite sandwich at  $y=L/2$ .

Although the HLM1 model computes accurate axial stress distributions, one can observe that the solutions for the transverse stresses oscillate around those of the elasticity theory, being this effect more evident towards the external layers. In view of the results, it is possible to state that the use of independent LW assumptions for displacements and stresses has proven to be a suitable choice for the accurate computation of the stress solutions in generic laminated structures, at the expense of extra degrees of freedom for the transverse stress fields.

### C. Free-edge in 3D laminated beam

The last numerical test is included with the aim of showing the advanced 3D capabilities of the proposed beam model. Axial extension is applied to a cross-ply beam and the free-edge effects that arise due to the mismatch of the mechanical properties of the plies at the interfaces of the laminae are analyzed. The accurate prediction of the interlaminar stresses is essential in these kind of structures due to their relation with free-edge delamination, which bring the composite structure to failure. CLT cannot capture this complex effects and, therefore, researchers usually rely on close-form solutions to approximate the elasticity solutions or finite element models with very refined meshes towards the edges, which result in much higher computational costs and the impossibility of dealing with real-life structures. With the proposed model, the intention is to tackle this issues and provide a tool to compute efficiently the stress fields for generic laminate problems, saltisfying *a priori* the ZZ and IC conditions, and keeping the computational costs a fraction of those of conventional solid models.

The problem case is generated to satisfy the assumptions taken in the pioneering work of Pipes and Pagano [50] on

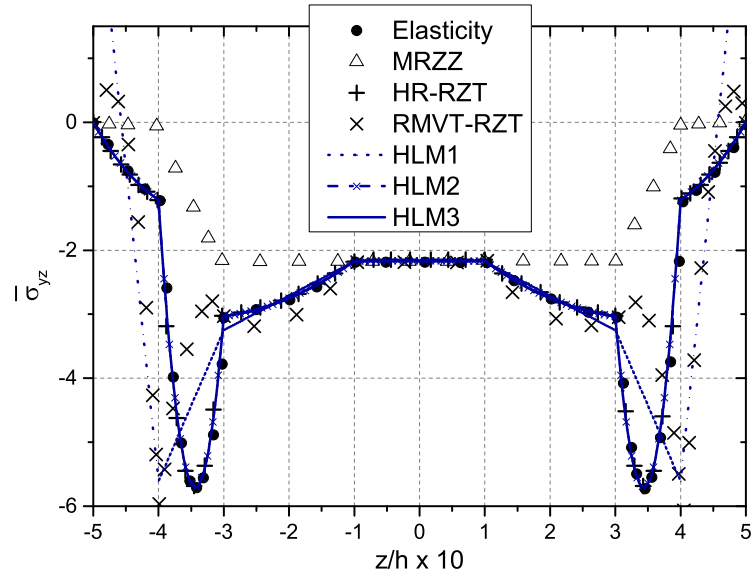


Fig. 13 Transverse shear stress of the composite sandwich at  $y=0$ .

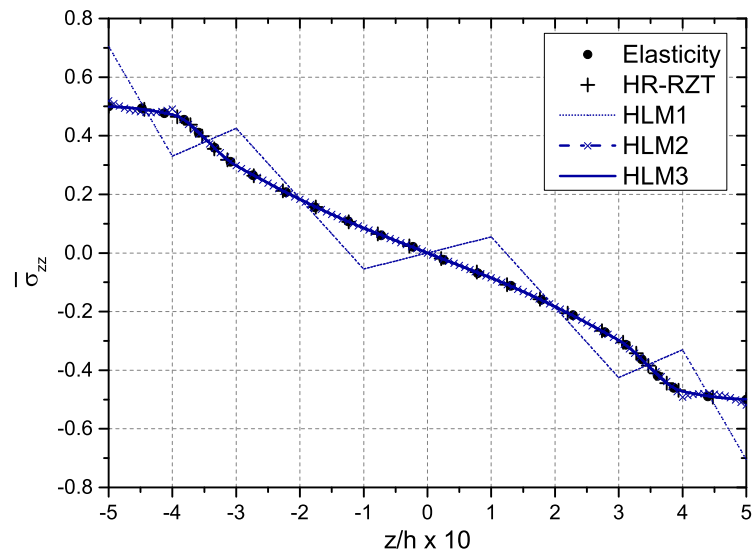
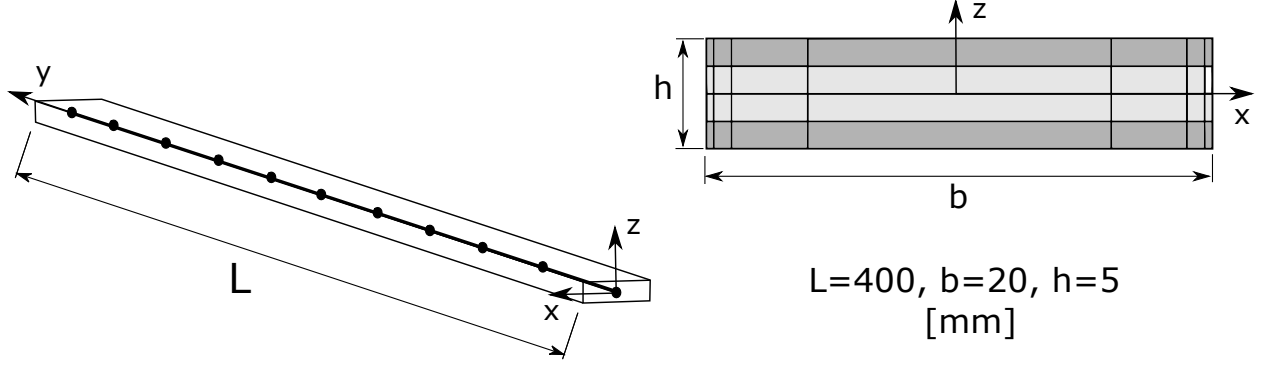


Fig. 14 Transverse normal stress of the composite sandwich at  $y=0$ .



**Fig. 15 Geometry and mesh of the laminated beam under axial extension.**

free-edge analysis. Accordingly, the mechanical properties of the material are:

$$E_1 = 137.9, E_2 = E_3 = 14.5, G_{12} = G_{13} = G_{23} = 5.9, \nu_{12} = \nu_{13} = \nu_{23} = 0.21 \quad (30)$$

( $E_i$  and  $G_{ij}$  in GPa). The stacking sequence is  $[45, -45]_S$  with all the layers of equal thickness and a global strain of magnitude  $\varepsilon_{yy} = \varepsilon_0 = 0.01$  is applied. The geometry and mesh of the model is shown in Fig. 15. The length-to-width ratio of the structure is  $L/b = 50$  and the width-to-thickness ratio is equal to  $b/h = 5$ . Ten cubic beam elements are employed for the finite element discretization and a distribution of HLE domains are generated over the cross-section surface. As mentioned before, one of the advantages of HLE models in composite simulation is that an arbitrary distribution of the expansion domains can be selected to represent the cross-section surface, allowing the user to refine the kinematics of the beam model in the critical zones (in this case at free-edges), as shown in Fig. 15 right.

Figure 16 shows the interlaminar shear stresses at  $y = L/2$ . One can notice that the approximated elasticity solutions of Pipes and Pagano [51] are properly represented if a sufficiently high polynomial order is employed for the stress assumptions over the section (HLM5). Figure 17 includes the shear stress distribution across the thickness of the laminate at the free-edge for different mixed and displacement-based models. Finally, the dependency between the width of the boundary layer where the free-edge effects arise and the thickness of the laminate is highlighted in Fig. 18, which shows the interlaminar shear stresses for thicknesses equal to  $h$ ,  $h/2$  and  $h/3$ .

## VI. Conclusions

A mixed beam element with 3D capabilities which is based upon the RMVT principle is proposed for the stress analysis of multilayered structures. In problems featuring one the geometrical dimensions greater than the other two, beam models present a major advantage in terms of computational costs in comparison to shell and solid finite element formulations. By using a refined LW theory of structure based on Legendre polynomials, known as the Hierarchical Legendre Expansions, the range of applicability of beam models can be extended to generic laminate problems, obtaining

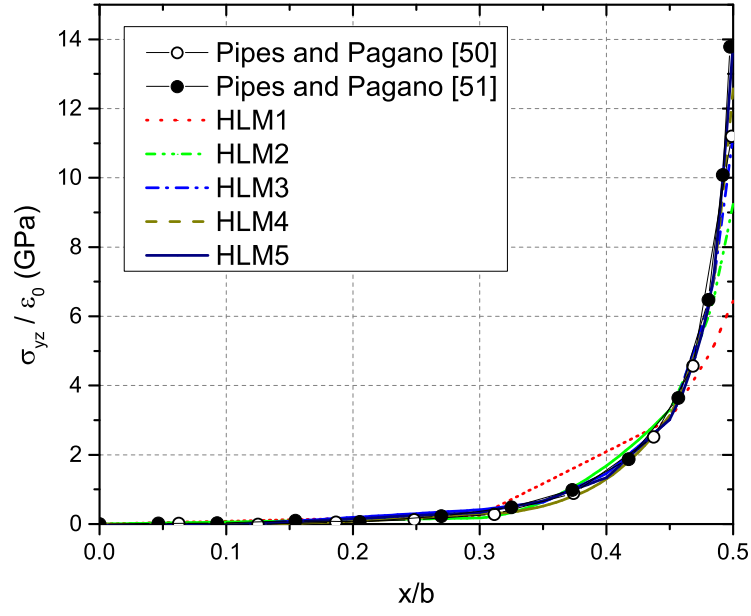


**Fig. 16** Transverse shear stresses along  $x$  at  $y=L/2$  and  $z=h/4$ .

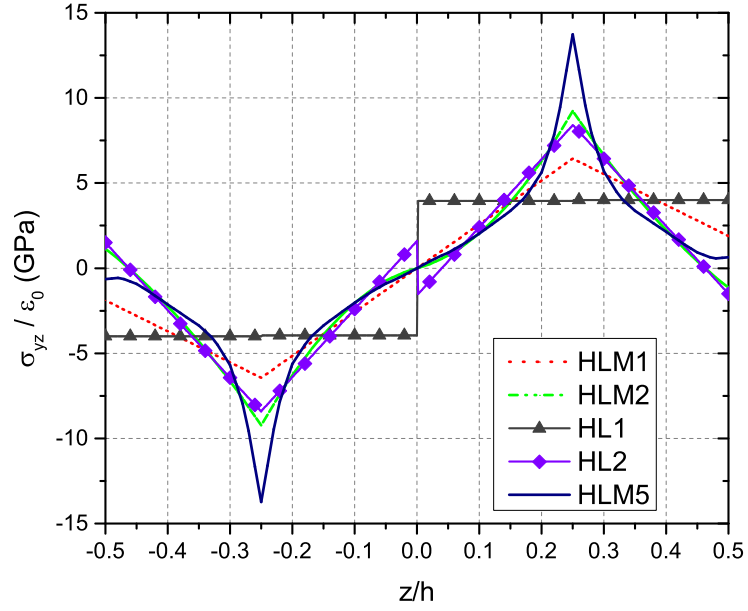


**Fig. 17** Transverse shear stresses along  $z$  at  $y=L/2$  and  $x=b/2$ .

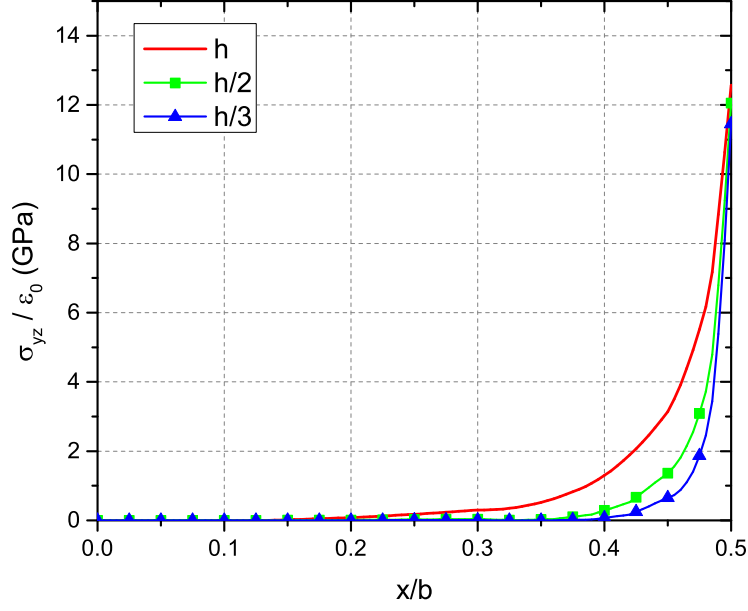


**Fig. 18** Transverse shear stresses along  $x$  for different thicknesses.

solid-like levels of accuracy in the computation of the stress solutions.

The RMVT can be considered as a natural extension of the PVD to multilayered problems, leading to a formulation in which the  $ZZ$  effects and the IC at the interfaces is satisfied *a priori* by independent assumptions of the transverse stress fields. This work has been focused on the assessment of the proposed 3D mixed beam element through benchmark solutions, with very satisfactory results. The results open the path for further investigations and developments of the model, such as dynamic analysis, non-linear problems and curved geometries, among others. Also, the static condensation of the stiffness matrices to obtain a class of mixed model with only displacement variables is worth of future investigation.



## Appendix

### A. Fundamental nuclei of RMVT-based beam elements

The explicit expressions of the components of the  $3 \times 3$  fundamental nuclei of the stiffness matrix,  $K_{uu}^{\tau sij}$ ,  $K_{u\sigma}^{\tau sij}$ ,  $K_{\sigma u}^{\tau sij}$  and  $K_{\sigma\sigma}^{\tau sij}$ , are reported in the following:

$$\begin{aligned}
K_{uu}^{\tau sij}(1, 1) &= C_{22} I_{ij} \int_{\Omega} F_{\tau,x} F_{s,x} d\Omega + C_{26} I_{i,y,j} \int_{\Omega} F_{\tau} F_{s,x} d\Omega + C_{26} I_{ij,y} \int_{\Omega} F_{\tau,x} F_s d\Omega + \\
&\quad C_{66} I_{i,y,j,y} \int_{\Omega} F_{\tau} F_s d\Omega \\
K_{uu}^{\tau sij}(1, 2) &= C_{26} I_{ij} \int_{\Omega} F_{\tau,x} F_{s,x} d\Omega + C_{66} I_{i,y,j} \int_{\Omega} F_{\tau} F_{s,x} d\Omega + C_{12} I_{ij,y} \int_{\Omega} F_{\tau,x} F_s d\Omega + \\
&\quad C_{16} I_{i,y,j,y} \int_{\Omega} F_{\tau} F_s d\Omega \\
K_{uu}^{\tau sij}(1, 3) &= 0 \\
K_{uu}^{\tau sij}(2, 1) &= C_{26} I_{ij} \int_{\Omega} F_{\tau,x} F_{s,x} d\Omega + C_{12} I_{i,y,j} \int_{\Omega} F_{\tau} F_{s,x} d\Omega + C_{66} I_{ij,y} \int_{\Omega} F_{\tau,x} F_s d\Omega + \\
&\quad C_{16} I_{i,y,j,y} \int_{\Omega} F_{\tau} F_s d\Omega \\
K_{uu}^{\tau sij}(2, 2) &= C_{66} I_{ij} \int_{\Omega} F_{\tau,x} F_{s,x} d\Omega + C_{16} I_{i,y,j} \int_{\Omega} F_{\tau} F_{s,x} d\Omega + C_{16} I_{ij,y} \int_{\Omega} F_{\tau,x} F_s d\Omega + \\
&\quad C_{11} I_{i,y,j,y} \int_{\Omega} F_{\tau} F_s d\Omega \\
K_{uu}^{\tau sij}(2, 3) &= 0 \\
K_{uu}^{\tau sij}(3, 1) &= 0 \\
K_{uu}^{\tau sij}(3, 2) &= 0 \\
K_{uu}^{\tau sij}(3, 3) &= 0
\end{aligned} \tag{31}$$

$$K_{u\sigma}^{\tau s ij}(1,1) = C_{23} I_{ij} \int_{\Omega} F_{\tau,x} G_s d\Omega + C_{36} I_{i,yj} \int_{\Omega} F_{\tau} G_s d\Omega$$

$$K_{u\sigma}^{\tau s ij}(1,2) = I_{ij} \int_{\Omega} F_{\tau} G_{s,z} d\Omega$$

$$K_{u\sigma}^{\tau s ij}(1,3) = 0$$

$$K_{u\sigma}^{\tau s ij}(2,1) = C_{36} I_{ij} \int_{\Omega} F_{\tau,x} G_s d\Omega + C_{13} I_{i,yj} \int_{\Omega} F_{\tau} G_s d\Omega$$

$$K_{u\sigma}^{\tau s ij}(2,2) = 0$$

$$K_{u\sigma}^{\tau s ij}(2,3) = I_{ij} \int_{\Omega} F_{\tau,z} G_s d\Omega$$

$$K_{u\sigma}^{\tau s ij}(3,1) = I_{ij} \int_{\Omega} F_{\tau,z} G_s d\Omega$$

$$K_{u\sigma}^{\tau s ij}(3,2) = I_{ij} \int_{\Omega} F_{\tau,x} G_s d\Omega$$

$$K_{u\sigma}^{\tau s ij}(3,3) = I_{i,yj} \int_{\Omega} F_{\tau} G_s d\Omega$$

(32)

$$\begin{aligned}
K_{\sigma u}^{\tau s i j}(1,1) &= -C_{23} I_{ij} \int_{\Omega} G_{\tau} F_{s,x} d\Omega + -C_{36} I_{ij,y} \int_{\Omega} G_{\tau} F_s d\Omega \\
K_{\sigma u}^{\tau s i j}(1,2) &= -C_{36} I_{ij} \int_{\Omega} G_{\tau} F_{s,x} d\Omega + -C_{13} I_{ij,y} \int_{\Omega} G_{\tau} F_s d\Omega \\
K_{\sigma u}^{\tau s i j}(1,3) &= I_{ij} \int_{\Omega} G_{\tau} F_{s,z} d\Omega \\
K_{\sigma u}^{\tau s i j}(2,1) &= I_{ij} \int_{\Omega} G_{\tau} F_{s,z} d\Omega \\
K_{\sigma u}^{\tau s i j}(2,2) &= 0 \\
K_{\sigma u}^{\tau s i j}(2,3) &= I_{ij} \int_{\Omega} G_{\tau} F_{s,x} d\Omega \\
K_{\sigma u}^{\tau s i j}(3,1) &= 0 \\
K_{\sigma u}^{\tau s i j}(3,2) &= I_{ij} \int_{\Omega} G_{\tau} F_{s,z} d\Omega \\
K_{\sigma u}^{\tau s i j}(3,3) &= I_{ij,y} \int_{\Omega} G_{\tau} F_s d\Omega
\end{aligned} \tag{33}$$

$$\begin{aligned}
K_{\sigma\sigma}^{\tau s ij}(1,1) &= -C_{33} I_{ij} \int_{\Omega} G_{\tau} G_s d\Omega \\
K_{\sigma\sigma}^{\tau s ij}(1,2) &= 0 \\
K_{\sigma\sigma}^{\tau s ij}(1,3) &= 0 \\
K_{\sigma\sigma}^{\tau s ij}(2,1) &= 0 \\
K_{\sigma\sigma}^{\tau s ij}(2,2) &= -C_{44} I_{ij} \int_{\Omega} G_{\tau} G_s d\Omega \\
K_{\sigma\sigma}^{\tau s ij}(2,3) &= -C_{45} I_{ij} \int_{\Omega} G_{\tau} G_s d\Omega \\
K_{\sigma\sigma}^{\tau s ij}(3,1) &= 0 \\
K_{\sigma\sigma}^{\tau s ij}(3,2) &= -C_{45} I_{ij} \int_{\Omega} G_{\tau} G_s d\Omega \\
K_{\sigma\sigma}^{\tau s ij}(3,3) &= -C_{55} I_{ij} \int_{\Omega} G_{\tau} G_s d\Omega
\end{aligned} \tag{34}$$

The  $I$  terms correspond to the integrals of the shape functions along the length of the beam element,  $l$ :

$$\begin{aligned}
I_{ij} &= \int_l N_i N_j dy \\
I_{i,yj} &= \int_l N_{i,y} N_j dy \\
I_{ij,y} &= \int_l N_i N_{j,y} dy \\
I_{i,yj,y} &= \int_l N_{i,y} N_{j,y} dy
\end{aligned} \tag{35}$$

All the integrals are computed using standard Gaussian quadrature.

## Acknowledgments

This research has been carried out within the project FULLCOMP - FULLy analysis, design, manufacturing, and health monitoring of COMPOSITE structures - funded by the Marie Skłodowska-Curie actions grant agreement no. 642121. The H2020 European Training Networks are gratefully acknowledged.

## References

- [1] Reissner, E., "On a certain mixed variational theorem and a proposed application," *International Journal for Numerical Methods in Engineering*, Vol. 20, No. 7, 1984, pp. 1366–1368. doi:10.1002/nme.1620200714.
- [2] Tsai, S. W., *Composites Design*, 4<sup>th</sup> ed., Dayton, Think Composites, 1988.
- [3] Reddy, J. N., *Mechanics of laminated composite plates and shells. Theory and Analysis*, 2<sup>nd</sup> ed., CRC Press, 2004.
- [4] Carrera, E., "C0 Reissner-Mindlin multilayered plate elements including zig-zag and interlaminar stress continuity," *International Journal for Numerical Methods in Engineering*, Vol. 39, No. 11, 1996, pp. 1797–1820. doi:10.1002/(SICI)1097-0207(19960615)39:11<1797::AID-NME928>3.0.CO;2-W.
- [5] Carrera, E., "C0z requirements - models for the two dimensional analysis of multilayered structures," *Composite Structures*, Vol. 37, No. 3, 1997, pp. 373 – 383. doi:10.1016/S0263-8223(98)80005-6, URL <http://www.sciencedirect.com/science/article/pii/S0263822398800056>.
- [6] Jones, R. M., *Mechanics of composite materials*, 2<sup>nd</sup> ed., Taylor and Francis Ltd., London, UK, 1998.
- [7] Timoshenko, S. P., "On the transverse vibrations of bars of uniform cross section," *Philosophical Magazine*, Vol. 43, 1922, pp. 125–131. doi:10.1080/14786442208633855.
- [8] Whitney, J., "The Effect of Transverse Shear Deformation on the Bending of Laminated Plates," *Journal of Composite Materials*, Vol. 3, No. 3, 1969, pp. 534–547. doi:10.1177/002199836900300316, URL <http://dx.doi.org/10.1177/002199836900300316>.
- [9] Mindlin, R. D., "Influence of Rotary Inertia and Shear on Flexural Motions of Isotropic, Elastic Plates," *Journal of Applied Mechanics*, Vol. 18, No. 1, 1951, pp. 31 – 38.
- [10] Lo, K., Christensen, R., and Wu, E., "A high-order theory of plate deformation. Part 2: laminated plates," *Journal of Applied Mechanics*, Vol. 44, 1977, p. 669. doi:10.1115/1.3424155.
- [11] Vlasov, V., *Thin-walled elastic beams*, National Technical Information Service, 1984.
- [12] Reddy, J., "A refined nonlinear theory of plates with transverse shear deformation," *International Journal of Solids and Structures*, Vol. 20, No. 9, 1984, pp. 881 – 896. doi:10.1016/0020-7683(84)90056-8, URL <http://www.sciencedirect.com/science/article/pii/0020768384900568>.
- [13] Lekhnitskii, S. G., "Strength calculation of composite beams," *Vestn. Inzh. Tekh*, Vol. 9, 1935.
- [14] Ambartsumian, S., "On a general theory of anisotropic shells," *Journal of Applied Mathematics and Mechanics*, Vol. 22, No. 2, 1958, pp. 305 – 319. doi:10.1016/0021-8928(58)90108-4, URL <http://www.sciencedirect.com/science/article/pii/0021892858901084>.

- [15] Murakami, H., "Laminated Composite Plate Theory With Improved In-Plane Responses," *Journal of Applied Mechanics*, Vol. 53, No. 3, 1986, pp. 661 – 666. doi:10.1115/1.3171828.
- [16] Reddy, J. N., "A generalization of two-dimensional theories of laminated composite plates," *Communications in Applied Numerical Methods*, Vol. 3, No. 3, 1987, pp. 173–180. doi:10.1002/cnm.1630030303, URL <http://dx.doi.org/10.1002/cnm.1630030303>.
- [17] Pagano, N., "Exact Solutions for Composite Laminates in Cylindrical Bending," *Journal of Composite Materials*, Vol. 3, No. 3, 1969, pp. 398–411. doi:10.1177/002199836900300304, URL <http://jcm.sagepub.com/content/3/3/398.abstract>.
- [18] Shimpi, R. P., and Ghugal, Y. M., "A new layerwise trigonometric shear deformation theory for two-layered cross-ply beams," *Composites Science and Technology*, Vol. 61, No. 9, 2001, pp. 1271 – 1283. doi:10.1016/S0266-3538(01)00024-0, URL <http://www.sciencedirect.com/science/article/pii/S0266353801000240>.
- [19] Surana, K., and Nguyen, S., "Two-dimensional curved beam element with higher-order hierarchical transverse approximation for laminated composites," *Computers and Structures*, Vol. 36, No. 3, 1990, pp. 499 – 511. doi:10.1016/0045-7949(90)90284-9, URL <http://www.sciencedirect.com/science/article/pii/0045794990902849>.
- [20] Carrera, E., "Theories and finite elements for multilayered, anisotropic, composite plates and shells," *Archives of Computational Methods in Engineering*, Vol. 9, No. 2, 2002, pp. 87–140. doi:10.1007/BF02736649.
- [21] Engrand, D., "Local Effects Calculations in Composite Plates by a Boundary Layer Method," *Local Effects in the Analysis of Structures*, Studies in Applied Mechanics, Vol. 12, edited by P. Ladevèze, Elsevier, 1985, pp. 199 – 214. doi:10.1016/B978-0-444-42520-1.50013-X, URL <http://www.sciencedirect.com/science/article/pii/B978044442520150013X>.
- [22] Noor, A. K., and Burton, W. S., "Stress and free vibration analyses of multilayered composite plates," *Composite Structures*, Vol. 11, No. 3, 1989, pp. 183 – 204. doi:10.1016/0263-8223(89)90058-5, URL <http://www.sciencedirect.com/science/article/pii/0263822389900585>.
- [23] Malik, M., and Bert, C. W., "Differential Quadrature Analysis of Free Vibration of Symmetric Cross-Ply Laminates with Shear Deformation and Rotatory Inertia," *Shock and Vibration*, Vol. 2, No. 4, 1995, pp. 321 – 338. doi:10.3233/SAV-1995-2406.
- [24] Reissner, E., "On a mixed variational theorem and on shear deformable plate theory," *International Journal for Numerical Methods in Engineering*, Vol. 23, No. 2, 1986, pp. 193–198. doi:10.1002/nme.1620230203, URL <http://dx.doi.org/10.1002/nme.1620230203>.
- [25] Reissner, E., *On a Certain Mixed Variational Theorem and on Laminated Elastic Shell Theory*, Springer Berlin Heidelberg, Berlin, Heidelberg, 1986, pp. 17–27. doi:10.1007/978-3-642-83040-2\_2, URL [http://dx.doi.org/10.1007/978-3-642-83040-2\\_2](http://dx.doi.org/10.1007/978-3-642-83040-2_2).
- [26] Toledano, A., and Murakami, H., "A high-order laminated plate theory with improved in-plane responses," *International Journal of Solids and Structures*, Vol. 23, No. 1, 1987, pp. 111 – 131. doi:10.1016/0020-7683(87)90034-5, URL <http://www.sciencedirect.com/science/article/pii/0020768387900345>.

- [27] Carrera, E., "Evaluation of Layerwise Mixed Theories for Laminated Plates Analysis," *AIAA Journal*, Vol. 36, No. 5, 1998, pp. 830–839. doi:10.2514/2.444.
- [28] Carrera, E., "Multilayered Shell Theories Accounting for Layerwise Mixed Description, Part 1: Governing Equations," *AIAA Journal*, Vol. 37, No. 9, 1999, pp. 1107 – 1116. doi:10.2514/2.821.
- [29] Carrera, E., "An assessment of mixed and classical theories on global and local response of multilayered orthotropic plates," *Composite Structures*, Vol. 50, No. 2, 2000, pp. 183 – 198. doi:10.1016/S0263-8223(00)00099-4, URL <http://www.sciencedirect.com/science/article/pii/S0263822300000994>.
- [30] Jing, H.-S., and Liao, M.-L., "Partial hybrid stress element for the analysis of thick laminated composite plates," *International Journal for Numerical Methods in Engineering*, Vol. 28, No. 12, 1989, pp. 2813–2827. doi:10.1002/nme.1620281207, URL <http://dx.doi.org/10.1002/nme.1620281207>.
- [31] Rao, K. M., and Meyer-Piening, H.-R., "Analysis of thick laminated anisotropic composite plates by the finite element method," *Composite Structures*, Vol. 15, No. 3, 1990, pp. 185 – 213. doi:10.1016/0263-8223(90)90031-9, URL <http://www.sciencedirect.com/science/article/pii/0263822390900319>.
- [32] Carrera, E., and Demasi, L., "Two Benchmarks to Assess Two-Dimensional Theories of Sandwich, Composite Plates," *AIAA Journal*, Vol. 41, No. 7, 2003, pp. 1356 – 1362. doi:10.2514/2.2081.
- [33] Wu, C.-P., and Li, H.-Y., "An RMVT-based third-order shear deformation theory of multilayered functionally graded material plates," *Composite Structures*, Vol. 92, No. 10, 2010, pp. 2591 – 2605. doi:10.1016/j.compstruct.2010.01.022, URL <http://www.sciencedirect.com/science/article/pii/S0263822310000528>.
- [34] Tessler, A., "Refined zigzag theory for homogeneous, laminated composite, and sandwich beams derived from Reissner's mixed variational principle," *Meccanica*, Vol. 50, No. 10, 2015, pp. 2621–2648. doi:10.1007/s11012-015-0222-0, URL <https://doi.org/10.1007/s11012-015-0222-0>.
- [35] Carrera, E., "Developments, ideas, and evaluations based upon Reissner's Mixed Variational Theorem in the modeling of multilayered plates and shells," *Applied Mechanics Reviews*, Vol. 54, 2001, pp. 301 – 329. doi:10.1115/1.1385512, URL <http://dx.doi.org/10.1115/1.1385512>.
- [36] Whitney, J. M., "Stress Analysis of Thick Laminated Composite and Sandwich Plates," *Journal of Composite Materials*, Vol. 6, No. 3, 1972, pp. 426–440. doi:10.1177/002199837200600301, URL <http://dx.doi.org/10.1177/002199837200600301>.
- [37] Washizu, K., *Variational Methods in Elasticity and Plasticity*, Pergamon Press, N.Y., 1988.
- [38] Reissner, E., "On the Theory of Bending of Elastic Plates," *Journal of Mathematics and Physics*, Vol. 23, No. 1-4, 1944, pp. 184–191. doi:10.1002/sapm1944231184, URL <http://dx.doi.org/10.1002/sapm1944231184>.
- [39] Murakami, H., Reissner, E., and Yamakawa, J., "Anisotropic Beam Theories With Shear Deformation," *Journal of Applied Mechanics*, Vol. 63, No. 3, 1996, pp. 660 – 668. doi:10.1115/1.2823347.

- [40] Murakami, H., and Yamakawa, J., “Dynamic Response of Plane Anisotropic Beams with Shear Deformation,” *Journal of Engineering Mechanics*, Vol. 123, No. 12, 1997, pp. 1268–1275. doi:10.1061/(ASCE)0733-9399(1997)123:12(1268).
- [41] E. Carrera, M. P., G. Giunta, *Beam structures: classical and advanced theories*, John Wiley and Sons, 2011.
- [42] Carrera, E., Filippi, M., and Zappino, E., “Laminated beam analysis by polynomial, trigonometric, exponential and zig-zag theories,” *European Journal of Mechanics - A/Solids*, Vol. 41, 2013, pp. 58 – 69. doi:10.1016/j.euromechsol.2013.02.006, URL <http://www.sciencedirect.com/science/article/pii/S0997753813000272>.
- [43] Szabó, B., and Babuška, I., *Finite Element Analysis*, John Wiley and Sons, Ltd, 1991.
- [44] Carrera, E., de Miguel, A., and Pagani, A., “Hierarchical theories of structures based on Legendre polynomial expansions with finite element applications,” *International Journal of Mechanical Sciences*, Vol. 120, 2017, pp. 286 – 300. doi: 10.1016/j.ijmecsci.2016.10.009, URL <http://www.sciencedirect.com/science/article/pii/S0020740316304088>.
- [45] Pagani, A., de Miguel, A., Petrolo, M., and Carrera, E., “Analysis of laminated beams via Unified Formulation and Legendre polynomial expansions,” *Composite Structures*, 2016. doi:10.1016/j.compstruct.2016.01.095, URL <http://www.sciencedirect.com/science/article/pii/S0263822316001185>, in press.
- [46] Pagano, N., “Influence of Shear Coupling in Cylindrical Bending of Anisotropic Laminates,” *Journal of Composite Materials*, Vol. 4, No. 3, 1970, pp. 330–343. doi:10.1177/002199837000400305, URL <https://doi.org/10.1177/002199837000400305>.
- [47] Carrera, E., and Demasi, L., “Classical and advanced multilayered plate elements based upon PVD and RMVT. Part 1: Derivation of finite element matrices,” *International Journal for Numerical Methods in Engineering*, Vol. 55, No. 2, 2002, pp. 191–231. doi:10.1002/nme.492, URL <http://dx.doi.org/10.1002/nme.492>.
- [48] Groh, R., and Weaver, P., “On displacement-based and mixed-variational equivalent single layer theories for modelling highly heterogeneous laminated beams,” *International Journal of Solids and Structures*, Vol. 59, No. Supplement C, 2015, pp. 147 – 170. doi:10.1016/j.ijsolstr.2015.01.020, URL <http://www.sciencedirect.com/science/article/pii/S0020768315000311>.
- [49] Tessler, A., Di Sciuva, M., and Gherlone, M., “Refinement of Timoshenko beam theory for composite and sandwich beams using zigzag kinematics,” Tech. Rep. 215086, National Aeronautics and Space Administration, 2007.
- [50] Pipes, R., and Pagano, N., “Interlaminar Stresses in Composite Laminates Under Uniform Axial Extension,” *Journal of Composite Materials*, Vol. 4, No. 4, 1970, pp. 538–548. doi:10.1177/002199837000400409, URL <https://doi.org/10.1177/002199837000400409>.
- [51] Pipes, R., and Pagano, N., “Interlaminar Stresses in Composite Laminates - An Approximate Elasticity Solution,” *Journal of Applied Mechanics*, Vol. 41, No. 3, 1974, pp. 668–672. doi:10.1115/1.3423368.